Modeling Pedestrian Crossing Paths at Unmarked Roadways

Xiangling Zhuang and Changxu Wu, *Member, IEEE*

***Abstract*—At the unmarked roadway, pedestrians cross the road with changing speeds and directions that result in curved paths and high chances of road accidents. However, few computational models have been built to address the mechanisms underlying the curved paths in crossing unmarked roadways. To better understand pedestrian behaviors and finally facilitate their safety, this paper modeled pedestrian paths at the unmarked roadway as a result of the decision-making process in which pedestrians try to minimize discomfort by weighing perceived risk (PR) with efficiency. PR is assumed to come from vehicles and specific positions on the road. Efficiency is modeled by the deviation from destination. The modeling mechanisms are consistent with existing theories, enhancing the understanding of pedestrian crossing behavior mechanisms at the unmarked roadway rather than treating the crossing process as a black box. The observed 135 pedestrian paths at two unmarked roadways in the real world were compared with the model's predictions. The potential applications of the model in exploring pedestrian position distribution at a crossing site and improving pedestrian presentation in existing driving simulators and intelligent transportation systems are discussed, as well as its limitations.**

***Index Terms*—Human behavior modeling, pedestrian crossing paths, pedestrian safety, unmarked roadway.**

I. Introduction

An unmarked roadway is an arbitrary mid-block location without any crossing facilities (signals, markers, etc.). As in other crossing sites, the process of crossing the unmarked roadway can be divided into three phases: walking to the curb, waiting at the curb, and crossing the street [1], [2]. "Walking to the curb" can be quantified with pedestrian movement models on how to avoid obstacles to reach destinations (not necessarily in the road-crossing context). In the context of crossing, the "destination" of this phase means the start point of crossing. The social force model [3], [4], the discrete choice model [5], [6], and cellular automata and its extended models [7]–[9] are representative models of this category [10]. "Waiting at the curb" means that pedestrians stay at the curb and wait for a proper time to cross. Gap-acceptance-based models have been applied to this situation [11], [12] to model the time that the pedestrian will begin crossing. These models depict whether pedestrians accept or reject the available gaps between vehicles while waiting at the roadside. The given two phases have determined how pedestrian walk to the start position and the time to begin crossing, but do not go further to quantify how pedestrians cross the street after that, which is the third phase of road crossing and the focus of the present model.

The phase "crossing the street" is a major concern in pedestrian safety because most injuries happen in this phase. In fact, in studies modeling pedestrian risk exposure [13], [14], pedestrians were assumed to be only at risk when crossing a road. This phase is more complicated than both "free walking" and "waiting to cross" situations. First, crossing pedestrians have to deal with relatively fast moving vehicles rather than static obstacles, such as buildings. Second, it poses higher demand on the accuracy of judgment because a small fault may result in a severe accident. The consequence is more serious than bumping into static obstacles in the context of walking. Finally, waiting pedestrians only need to decide when to cross, but crossing pedestrians also need to consider direction and speed of crossing. These differences mean that, although models for the first two phases can be extended to the crossing phase (e.g., in [15]–[17]), much effort is still needed in modeling crossing behaviors, particularly in the third phase.

Pedestrian path modeling is a new topic in crossing behavior modeling. Since drivers and pedestrians are the two main users of the road, many pedestrian research topics are adapted from driver research, such as the gap acceptance theory [18], the hierarchy driving behavior model by Michon [19], and a phone-related distraction study [20]. Pedestrian path modeling, however, is beyond this scope as pedestrian behaviors distribute discretely over time [21], and they change speeds and directions very frequently. Moreover, compared with vehicles restricted to traveling within designated lanes, pedestrians' lateral positions at crossing sites are not as confined, resulting in very autonomous trajectories. This is particularly true at uncontrolled crossing sites such as unmarked roadways.

It should be noted that an unmarked roadway is different from a "shared space," which is a popular road design style that "minimizes demarcations between vehicles and pedestrians" [22]. The aim of shared space is to increase pedestrian priority [23], whereas pedestrians at the unmarked roadway are illegal road users with no priority and can thus receive no help from crossing facilities. Therefore, pedestrians at the unmarked roadway have to make crossing decisions (how to cross) autonomously and behave differently with their counterparts at other crossing sites. For instance, at signalized crosswalks, Geruschat *et al.* [1] found that pedestrians spent 13% of their

Manuscript received March 24, 2012; revised September 18, 2012, January 15, 2013, and April 1, 2013; accepted May 2, 2013. Date of publication July 9, 2013; date of current version August 28, 2013. This work was supported by the National Basic Research Program of China under Grant 2011CB302201. The Associate Editor for this paper was R. J. F. Rossetti.

X. Zhuang is with the Institute of Psychology, Chinese Academy of Sciences, Beijing 100101, China.

C. Wu is the corresponding author of this paper (e-mail: changxu.wu@gmail.com).

Color versions of one or more of the figures in this paper are available online at http://ieeexplore.ieee.org.

Digital Object Identifier 10.1109/TITS.2013.2267734

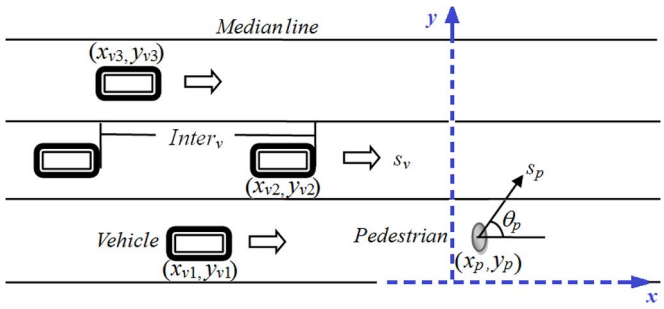

Fig. 1. Crossing situation and variables ($N = 6$).

crossing time checking the left and right directions. As a comparison, Zhuang and Wu [24] found a counterpart of 60% at an unmarked roadway. The difference is more prominent in terms of walking paths. Usually, pedestrians at legal crossing sites just follow the regulation and go toward their destinations, and the drivers will yield to them. The decision-making process in the rule-following behaviors is very simple. In contrast, at the unmarked roadway, pedestrians as illegal road users hesitate to force the drivers to yield to them. Instead, they yield to vehicles by stopping or changing directions, which is evidenced by more tortuous long paths than the straight short paths in observation [24]. The changeable behaviors from autonomous decision-making at the unmarked roadway are the first reason for giving special attention to this kind of crossing sites. Research on the unmarked roadway is also important for safety reasons. In many developing countries (e.g., China and Saudi Arabia), traffic laws are not well obeyed, and many people have died because of crossing roadways at illegal sites [25], [26]. In China, one accident report [26] shows that this reason leads to 3193 fatalities and 7123 injuries in 2004, ranking the highest among other pedestrian reasons that caused accidents. It is hoped that modeling pedestrian paths can facilitate our understanding of the mechanisms governing pedestrian behaviors and finally improve safety.

In summary, the previous related work on pedestrian modeling has not paid enough attention to the final phase of pedestrians' crossing behaviors in a context with moving vehicles and without restrictions from traffic signals. To fill this gap, this paper aims to model pedestrian crossing paths, which is an important aspect of crossing behaviors at unmarked roadways. The model can help to understand the computational mechanism of pedestrian road-crossing behaviors, and the generated path can be used to improve pedestrian research tools and systems for pedestrian protection. This paper is organized as follows: Section II describes the model formulation. Section III presents the model calibration with field data, and Section IV validates the field data. The discussion concludes this paper with the potential applications and limitations of the model.

II. Modeling Pedestrian Paths

A. Model Framework

Since the crossing process is considered to be composed of crossing two similar halves of the road (see the Appendix), the following will only show the path modeling of the first half of the road. As an example, Fig. 1 shows a pedestrian crossing one half of a six-lane road. If the crossing area is regarded as a coordinate plane, the pedestrian path is then a record of pedestrian positions, which can be represented by the coordinates. The y-axis starts at the roadside and the x-axis starts at the initial position of a pedestrian when he/she arrived at the crossing point. Pedestrian positions can be achieved by adding initial positions and distance walked afterward. With the variables shown in Fig. 1, pedestrian position at time nt is formulated as

$$x_p = x_p(0) + \sum_{j=1}^{n} s_{p_j} \cos \theta_{p_j} t \tag{1}$$

$$y_p = y_p(0) + \sum_{j=1}^{n} s_{p_j} \sin \theta_{p_j} t \tag{2}$$

where n denotes the nth time step, $x_p(0)$ and $y_p(0)$ are the initial coordinates of a pedestrian, and for all the pedestrians, $x_p(0) = 0$. $y_p(0)$ may not be equal to zero since pedestrians do not necessarily stay at the same starting place (i.e., the curb) before crossing.

The following aims to quantify s_p and θ_p in (1) and (2). The following is a list of variables to be used.

N	number of lanes in the road;
L	lane width [m];
t	time step (1 s);
$\boldsymbol{i}$	tag of road lane;
N_{group}	group size;
PRl	perceived risk (PR) for the current location;
PRv	PR for vehicles;
$\text{PRv}_{\boldsymbol{i}}$	PR for the first vehicle in lane i;
(x_p, y_p)	coordinate of the pedestrian;
$(x_{\boldsymbol{d}esti}, y_{\boldsymbol{d}esti})$	coordinates of the pedestrian destination;
(x_{vi}, y_{vi})	coordinates of the first vehicle v in lane i;
Inter_v	distance between a following vehicle and the lead vehicle in the same lane;
Δt_i	predicted time gap between the first vehicle in lane i and the pedestrian to arrive at their intersection point;
θ_p, θ_{vi}	angle between the road direction to the right and the velocity of the pedestrian (θ_p) or vehicle (θ_{vi}). θ_{vi} means the angle of the vehicle at lane i. It is 0 at the near side, and π at the far side of the road.

In a speed choice study of drivers, Tarko [27] used a subjective time value, perceived risk, and perceived enforcement of speed limits to represent trip disutility. Although pedestrians do not have speed limits corresponding to the last of the three components, the other two components were also important in the context of pedestrian road crossing. A subjective time value is the cost of travel time along the unit distance. This means that drivers want to maximize speed to reduce cost and to keep to their schedule. Perceived risk depends on the perception of crash risks along the road. Two similar concepts were mentioned in a comprehensive overview about pedestrian behaviors. Ishaque and Noland [28] found that pedestrian speed was a function of pedestrian capability, value of time, and risk evaluation, i.e.,

$$\text{Speed} = f(\text{Capacity, value of time, risk evaluation}). \tag{3}$$

Since the model mainly addresses the crossing path of an average pedestrian, capacity is not considered. The "value of time" represents the intolerance of delays. It is similar to the "time value" in [27] because both reflect the eagerness to move toward a destination. This component is included in the current model as one source of crossing discomfort. It is named "*distance deviation,*" and is formulated with the deviation of current position from a destination. Risk evaluation in (3) is the pedestrians' evaluation of the risk of their behaviors. It is similar to the perceived risk in [27] and is included here as another source of crossing discomfort.

It is assumed that pedestrians have expected discomfort of crossing in certain ways and choose the one with the minimum discomfort. This assumption follows the utility-based theories [29] and has been used in other pedestrian behavior modeling works [30]. Following this assumption and the previous findings given, pedestrian velocity can be considered as a function of "discomfort," which itself is determined by PR and distance deviation, i.e.,

$$\begin{aligned}\text{Velocity} &= g\ (\text{Discomfort}) \\ &= (\text{Perceived Risk} + \text{Distance deviation}). \end{aligned} \tag{4}$$

B. Perceived Risk

PR was assumed to consist of three components: threat from the vehicles, pedestrian location on the road, and group size. Clearly, pedestrian PR increases with higher risk from vehicles PRv and location-defined risk PRl. The two components have the same scale and unit; therefore, they were simply added. Group size acted as a moderator since pedestrians in bigger groups perceive less risk. According to Hamed [31], pedestrians in groups were more likely to cease waiting to begin crossing than individuals. Leden [32] also found that pedestrian risk decreased with increasing pedestrian flow. As bigger group size is usually related with higher pedestrian flow, this implied less risk for bigger group size. Given this, we have

$$\text{Perceived Risk} = a_g/N_{\text{group}} * (\text{PRv} + \text{PRl}) \tag{5}$$

where a_g is a coefficient adjusting the effect of group size.

1) PRv: The gap acceptance theory was partly adopted to model the PR. According to Das *et al.* [12], pedestrians have a critical gap in mind. Pedestrians predict the time gap between vehicles and themselves to arrive at an intersection point. If the time gap is bigger than their critical gap, they will cross. Therefore, pedestrian PR from vehicles decreases with increasing vehicle gaps, but it gradually converges to zero after the critical gap. Pedestrian acceptance is usually modeled by logistic regression. For instance, Brewer *et al.* [11] modeled the probability of accepting a gap in the following form (left side of"$\rightarrow$"):

$$p = \frac{e^{\beta \Delta T}}{1 + e^{\beta \Delta T}} * 100 \rightarrow \frac{1}{p} \propto e^{-\beta \Delta T}. \tag{6}$$

In (6), ΔT is the gap, and β is a parameter representing the strength of the relationship.

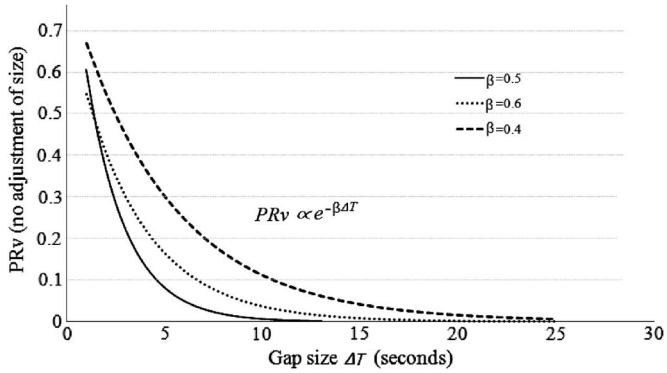

Fig. 2. Negative exponential relation between PRv and ΔT. The solid line shows the final formulation of PRv (before adjustment of size), whereas the dashed line is for comparison.

Since the probability of accepting a gap should be inversely proportional to the risk from the behavior ($1/p \propto$ PRv), PR from the vehicles should take the negative exponential form (PRv $\propto e^{-\beta \Delta T}$). Therefore, although Gupta *et al.* [33] suggested risk $= f(1/\text{gap})$ as the possible relationship, this model adopted the negative exponential form, as shown in Fig. 2.

PRv in Fig. 2 is pedestrians' PR from only one vehicle; the total PRv should incorporate more vehicles. The question is which vehicles should be incorporated in formulating PRv. Most pedestrian acceptance studies only consider the first approaching vehicle among all vehicles, regardless of which lane it is located, as in [12] and [16]. It is partly reasonable because, for a pedestrian standing still at the roadside (as in these studies), the position and speed of the headmost vehicle can reflect the upcoming danger. However, for pedestrians crossing the road, this kind of risk evaluation is insufficient. Brewer *et al.* [11] found a "rolling gap" phenomenon where, although crossing pedestrians evaluated vehicles of farther lanes, they mainly focused on one lane at a time in gap acceptance judgments. For instance, when crossing lane 1, although the gap produced by the headmost vehicle (in lane 3) is very small, they may still go ahead because the gap in lane 1 is big enough, and they anticipate that the vehicle would have passed when they arrive at lane 3. Judging from this, potential risk from both the headmost vehicle and the first vehicles in lanes nearby (more important) were evaluated by pedestrians when making decisions. To make the criteria more specific, in our model, the first vehicles meeting all the following criteria were included in calculating the PR from vehicles.

1) Vehicles are at the same half of the road with pedestrians.
2) Vehicles are in the lanes ahead of pedestrians.
3) Vehicles are approaching rather than leaving pedestrians.

Among these vehicles, we assume that the headmost vehicle in the lane right before the pedestrians has the largest weight. Once the headmost vehicle surpasses a pedestrian (judged from the comparison of pedestrian lateral positions x_{vi} and x_p), the closest following vehicle becomes the new vehicle to be considered.

The final formulation of PRv for all vehicles is

$$\text{PRv} = a_{\text{PRv}} \sum_{i \in K} \frac{e^{-0.5|\Delta T|}}{y_{vi} - y_p + 1}$$

$$K = \{y_p + w/2 \leqslant N/2^* L \text{ and } x_{vi} \leqslant x_p \text{ or } y_{vi} + w/2 \geqslant y_p \geqslant N/2^* L \text{ and } x_{vi} \geqslant x_p\}. \quad (7)$$

In (7), parameter a_{PRv} helps to unite the scale. Constraint K represents vehicles that have influence on pedestrians considering the vehicle width w. $y_{vi} - y_p + 1$ is the adjustment for the PR of vehicles not in the same lane with pedestrians since farther vehicles had smaller effects on pedestrians.

$e^{-0.5|\Delta T_i}$ is the negative exponential part in the equation, as shown in Fig. 2. Parameter β was estimated to be 0.5 based on literature.[1]

ΔT_i is the time gap between pedestrians and the vehicle to arrive at their interaction point (gap size). It is formulated as

$$\Delta T_i = \frac{|x_p - x_{vi}|}{s_{vi} \cos \theta_{vi} - s_p \cos \theta_p} - \frac{|y_{vi} - y_p|}{s_p \sin \theta_p}. \quad (8)$$

The distance between the vehicle and the pedestrian $(x_p - x_{vi})$ was put in the absolute value mark because $x_{vi} > x_p$ will be true at the far side of the road.

The position of vehicles (x_{vi}, y_{vi}) can be formulated similarly to that of the pedestrians in (1) and (2) with corresponding s_v and θ_{vi}. S_v and θ_{vi} are assumed to be constant to simplify the behaviors of the drivers, as in [12]. This constraint can be relaxed by extending the model in our future work (see Section V). The first difference with pedestrians' position formulation is that $y_{vi}(0)$ and $x_{vi}(0)$ are not equal to zero. $x_{vi}(0)$ is equal to the distance between the pedestrian and the influencing vehicle when they first arrived at the crossing point. $y_{vi}(0)$ is formulated as

$$y_{vi} = 0.5L + (i-1) * L. \quad (9)$$

Since only the first vehicle of one lane has influence on pedestrians, positions of vehicles must be updated based on the headway time gap between vehicles (Inter_v) when the initial first vehicle in that lane passed before pedestrians.

When the pedestrian speed in the direction of the y-axis is equal to zero (standstill or walk along the road), $s_p \sin \theta_p$ is equal to zero, and (8) will not stand. In this situation, if the pedestrian is within the range of a vehicle's future path $(y_{vi} - y_p < w/2$, where w is the vehicle width), (5) can be simplified to contain only the minuend; otherwise, $\Delta T_i = \infty$, which means $\text{PRv}_i = 0$.

[1]Sun *et al.* [16] observed that the critical gap for the individual pedestrian is 4.6 s and that for groups of 2 or 4 is 5.6 s, meaning that the curve has a rapid decrease around 5s and then becomes flat. Moreover, a study also conducted at unmarked roadways shows that the smallest gap that has 100% acceptance is 10 s [34], which means that PRv would approximate zero for gaps longer than 10 s. In summary, the function that can best satisfy all three constraints should get β as 0.5.

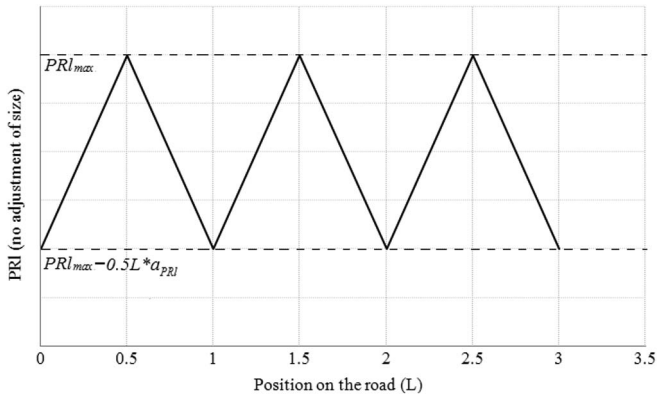

Fig. 3. Location-based risk perception. The x-axis is the position denoted by lanes on the road.

2) PRl: PRl in (5) is PR determined by locations on the road. Usually, a wide road is divided into several lanes and marked with white lines. Although vehicles can change lanes occasionally, they stick to one lane most of the time for safety [35]. Therefore, pedestrians have become accustomed to thinking that vehicles are more likely to be in the middle of one lane. Even when vehicles are not present, this effect may still exist. Consequently, it is assumed that the PR in the middle of one lane is the highest of the lane and that it decreases with the distance to the middle line. It should be noted that, although vehicles occupy a specific width, the entire road section within its width does not impose the same risk to pedestrians. It is natural for people to run to the nearest lane border to avoid approaching vehicles within a lane in the case of danger. Therefore, the closer an individual is to a vehicle's midline, the more difficult it is for the individual to run out of its threat zone. Consequently, it is still reasonable to assume that the risk decreases gradually with a larger distance from the middle line. For simplicity, the decline is assumed to be linear as in (10) and Fig. 3.

$$\text{PRl} = \text{PRl}_{\max} - a_{\text{PRl}} |y_p \% L - 0.5L|. \quad (10)$$

$\%$ is the modulus operator, and the section within the absolute mark represents pedestrians' distance to the center of the current lane. $\text{PRl}_{\max}$ is the PR in the middle of one lane and a_{PRl} is the slope of the risk as it varies with the positions on the road. The only constraint for (10) is that $\text{PRl}_{\max} > 0.5 \text{ L} * a_{\text{PRl}}$. Since both $PRl_{\max}$ and a_{PRl} are the parameters to be estimated and can be multiplied by a common factor, PRl was not assigned with an additional parameter to unite the scale as PRv.

C. Distance Deviation

If the PR was the only source of the crossing discomfort, pedestrians would simply wait at the roadside and never cross. This indicates that they also have a driving force to proceed toward the destination. Hamed [31] found that when pedestrians' waiting time increased, their attempts to cross increased. In addition, pedestrians who had waited longer at the roadside had a higher risk of ending their waiting time when they crossed from the central refuge to the other side of the road. These

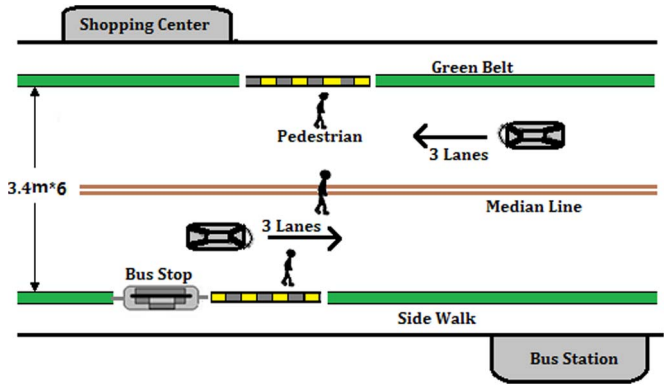

Fig. 4. Site for data collection (Hangzhou).

results showed that people have limited patience and implied that efficiency was valued in addition to safety. Therefore, discomfort caused by distance deviation is represented with the square of the difference between the current position and destination, i.e.,

$$a_{\text{deviation}}\left((x_p - x_{\text{desti}})^2 + y_{\text{deviation}}(y_p - y_{\text{desti}})^2\right). \quad (11)$$

$y_{\text{deviation}}$ is the weight of longitudinal deviation relative to lateral deviation. Since the most important task of "crossing a road" is to traverse the roadway, $y_{\text{deviation}}$ is assumed to be larger than one. Similar to a_{PRv}, $a_{\text{deviation}}$ is a coefficient to change the scale of variables and adjust the weight of *distance deviation* in discomfort.

III. Model Calibration

A. Data Collection

The field data for testing the model were collected at a typical unmarked roadway section near a bus station in Hangzhou, China (see Figs. 1 and 4 for the sketch of the roadway section). The two-way road has three lanes on each side with a lane width of 3.4 m. There are no raised median or green belt at the median line. Two synchronized cameras were set at both sides of the road. The first camera was set on a high-rise building to get the main situational and behavioral data, and the other camera is set beside the road to record the details for later check. On average, 757 pedestrians and 2826 vehicles used the site each hour within the observation phase, and the average vehicle speed was 7.3 m/s.

The collected videos were played back in Adobe Premiere Pro CS4 version 4.0.1 with time display accuracy of 0.04 s to get pedestrian-related data to be used as model input and output. The pedestrians were included in the sample on the order of their arrival time, as long as they met the following criteria. First, the pedestrians can be viewed in the camera clearly during the whole crossing process. Second, a pedestrian is either walking alone or within small groups that has fewer than 12 pedestrians. Finally, the traffic is smooth, and the road is not clear. For these pedestrians, their initial and target positions, i.e., positions every 1 s, group sizes, vehicle speeds, and time gaps between vehicles were collected. All the positions are coded manually based on road markers and lane width. As the model focuses on the average pedestrian crossing the street, demographical variations such as gender and age were not specially addressed. They follow the natural distribution in the field observation. Overall, 159 cases of pedestrians were coded, from which 54 cases were selected randomly for the calibration, and the left cases were left for validation.

B. Input of the Model and its Parameter Settings

The coordinates of pedestrian destinations, their original positions after arrival, and their group size were extracted from the calibration data set. The context related inputs are the number of lanes (6), lane width (3.4 m), initial position of headmost vehicles, vehicle speed, and time gap between vehicles. Vehicle width was set as 2 m based on the common width of a car.

Pedestrian speeds and directions were not the inputs of the model, but in order to provide the set of choices under the maximized utility framework, they were given to restrain the range of choices. Empirical pedestrian speeds were categorized into five subsets by getting the percentiles at every 20% of the instant speed set. When a certain level of speed was chosen in the computation, the final speed was generated with normal distribution subjected to the mean and standard deviation of the corresponding subset. Pedestrian directions were selected discretely from seven directions (0°, 30°, 60°, 90°, 120°, 150°, 180°). The seven choices are approximations and discretizations of pedestrian real direction choices. Additional directions were not included due to accuracy requirements in practical applications and computational efficiency considerations. A simple enumeration algorithm was used to get the optimal value for the five free parameters a_{PRv}, $a_{\text{deviation}}$, a_{PRl}, $\text{PRl}_{\max}$, and $y_{\text{deviation}}$. (Since a_{group} always come together with other parameters, it was set as one.) The criterion is to get the minimum overall root-mean-square error (RMSE) of the 54 pedestrians' observed and modeled paths.[2] The ranges of the parameters were first determined by the trial-and-error method and then determined by previous enumeration results, with smaller and smaller steps within the range. The final RMSE is 0.87 m in the calibration, and the average R^2 for 44 of all the cases is 0.70 (others cannot be calculated). The values for the parameters are shown in Table I.

IV. Model Validation

Except for the data set of 105 pedestrians obtained from the calibration site, 30 pedestrians crossing at another site were also included as validation samples to show the model's predictability at a different layout. The new site is near a subway station in Beijing, China (see Fig. 5 for the sketch of the new site).

[2]Since all pedestrians had the same longitudinal distance (i.e., road width) during the crossing, path fitness was measured by RMSE of the modeled and observed pedestrian lateral positions when they arrived at certain longitudinal positions (points uniformly distributed on the y-axis coordinate). These positions are selected every 0.2 m; therefore, each pedestrian has 102 positions to calculate the RMSE. R^2 is considered as a supporting fitness index because if pedestrians walk perpendicular to the road direction all the time, their lateral positions will remain constant, and consequently, the R^2 cannot be calculated.

TABLE I
FREE PARAMETER ESTIMATION RESULTS

Free Parameter	Description	Value
PRI_{max}	*PRI* at the middle line of one lane	3.5
a_{PRI}	Slope of *PRI* changing with distance to the middle of the lane	1.5
$y_{deviation}$	Weight of longitudinal deviation (relative to lateral) in "Deviation"	1.4
$a_{deviation}$	Weight of distance deviation (relative to *PR*) in "Discomfort"	1.5
a_{PRv}	Weight of *PRv* (relative to *PRI*) in "*PR*"	7

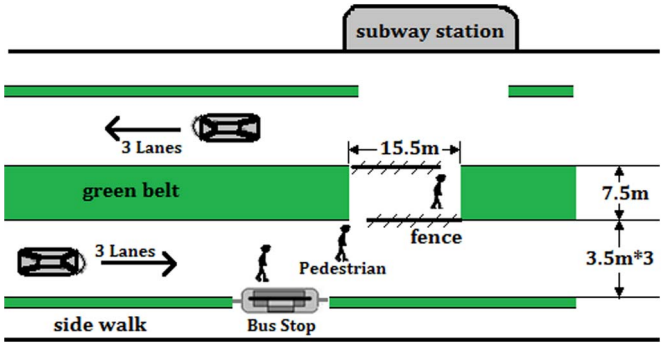

Fig. 5. Site 2 for validation data collection (Beijing). Only the lower half were considered in the data collection.

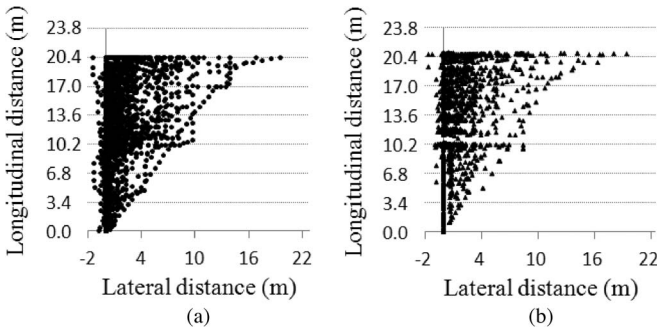

Fig. 6. Observed and modeled pedestrian position distribution. (a) Observation. (b) Model.

The six-lane road was divided by a road safety fence (15.5 m), which was removed a little (2 m) by pedestrians trying to cross there. Since there is a wide green belt with a width of 7.5 m in the middle of the road and the trees in the green belt are tall enough to block a pedestrian's view of the other side, only half of the road was included in the data collection, considering the half itself as a three-lane road. The "road" had 258 pedestrians and 1403 vehicles per hour, with an average vehicle speed of 12 m/s. Due to the differences between the two sites, the validation results could not be merged. However, the indexes to be compared are similar; therefore, only the validation results of site 1 (Hangzhou) were presented in detail, whereas those of site 2 (Beijing) in brief. This part first compared the modeled and observed position distribution on the road of the whole sample to get a rough view of the fitness. The path predicted for each pedestrian was then evaluated based on RMSE and R^2.

A. Position Distribution of the Whole Sample at Site 1

Fig. 6 shows the comparison of the modeled and empirical discrete positions from 105 pedestrians. The points can be viewed as pedestrian footprints. The model successfully

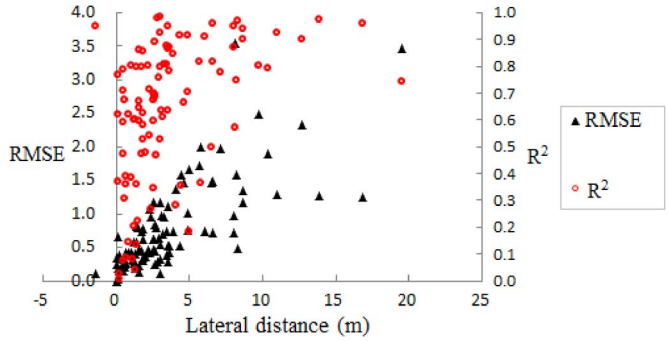

Fig. 7. RMSE and R^2 of pedestrians' modeled and observed paths.

repeated the empirical data in that both figures have dense footprints in the upper left of a square. The shape or outline is quite similar, and the edge of the y-axis has attracted most footprints. This indicates that pedestrians prefer to go straight and then turn to their destination rather than the other way around; otherwise, the footprints would distribute within the lower right of the square.

B. Path Fitness of Individual Pedestrians at Site 1

The preceding comparison of the positions for the whole sample offered fitness clues to the "average" pedestrian crossing model. This part evaluated the model with higher standards orienting to individual pedestrians, considering their start and end points. The overall RMSE of the lateral position of all cases is 0.98 m. Fig. 7 shows that as pedestrians' destinations become farther in the lateral direction, RMSEs have an increasing trend that indicates more difficult predictions. Most pedestrians, however, were predicted well with small RMSEs that were below 1 m. Overall, R^2 was calculated for 97 cases with a mean of 0.63.

Since the paths varied greatly with situations, a categorization of the pedestrian paths was conducted based on the path shapes. The iteration of classification ended up with five path types, as in Fig. 8. These paths are shown with a connection line between several critical points on the road. Point 1 is the start, whereas point "5" and "8" represents two kinds of destinations. Other points represent possible turning points of the pedestrians, with points 3 and 6 at the middle line of the road.

Type a: 1→5. Pedestrians go perpendicularly to the road toward their destinations (seven pedestrians) or deviate a short distance ($\leq$1 m) from that path (20 pedestrians).

Type b: 1→2→7→8. Pedestrians go perpendicularly to the road in the start and end sections, but in the middle section, they simply go directly toward the temporary destination.

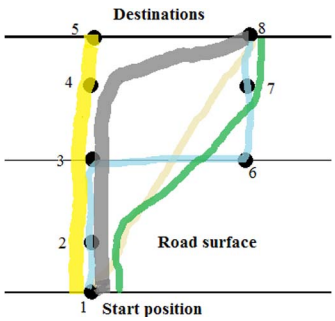

Legend	Path type	RMSE	R^2	Num of pedestrians
a	1→5	0.24	0.49	27
b	1→2→7→8	0.60	0.56	19
c	1→4→8	0.78	0.70	33
d	1→8	0.98	0.79	9
e	1→3→6→8	1.43	0.70	17

Fig. 8. Path types and model fitness of every type. The figure only shows the general pattern of the paths rather than specific paths with accurate turning positions. The black circles are some critical turning points that are usually located at the lane borders. Most pedestrians fall in Types a and c; therefore, they are shown in a thicker line than others. The points are turning points, but they do not necessarily locate as the figure shows.

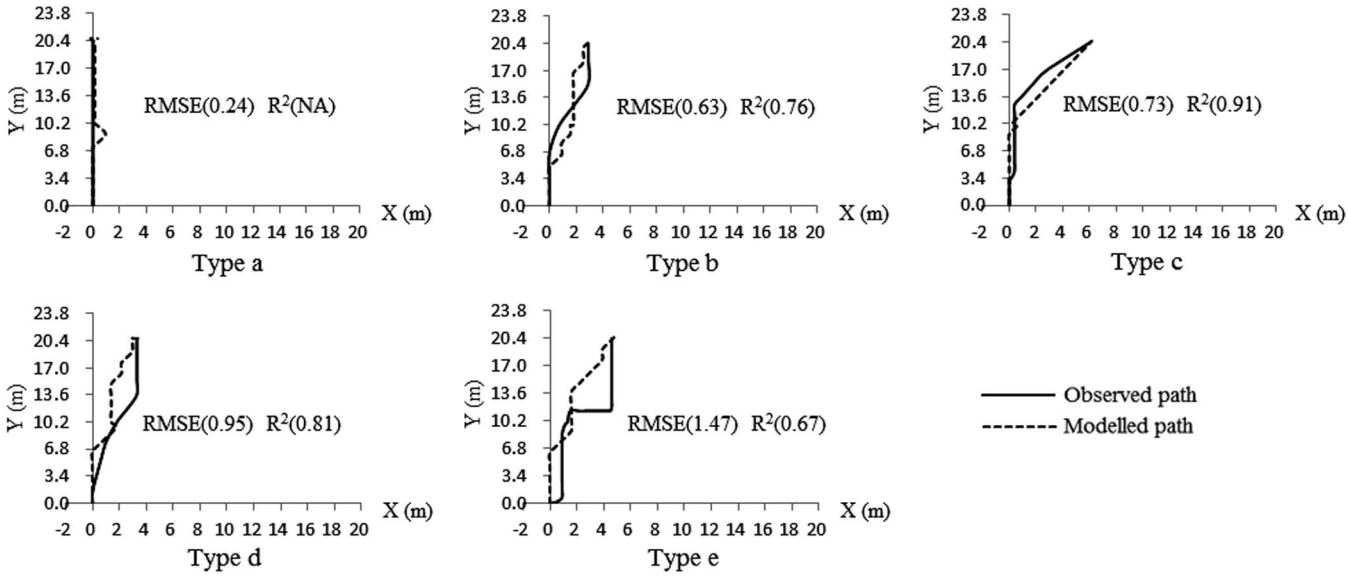

Fig. 9. Modeled (dash line) and observed (solid line) pedestrian path examples for five path types.

Type c: 1→4→8. At the fourth and fifth lanes, 24 of the 33 pedestrians turned to go directly toward their destinations.

Type d: 1→8. Similar to Type a, pedestrians go directly toward their destinations.

Type e: 1→3→6→8. Pedestrians go perpendicularly to the road to the middle line, go along the road, and repeat the first mode until they reach the destination.

For each path type, an example is shown in Fig. 9, comparing the observed and predicted paths. The cases were selected because its fitness is closest to the average fitness of the path type where it belongs. Type a has the smallest RMSE among all the types; however, it also has the lowest R^2 due to the limited variation in the lateral direction. The middle three types in Fig. 8 were predicted well with small RMSE and acceptable R^2. However, the Type e was not predicted well by the model. The very obvious turnings (two 90° turns) and long distance along the road may imply that pedestrians have two temporary destinations (3, 6) at the turning points, which are beyond the control of safety or efficiency. Without the extra input of transient destinations, the predicted paths always go directly to the final destination instead of turning to the temporary destination first (see Fig. 9).

C. Validation Results at Site 2

Although pedestrians at site 2 also prefer to go perpendicularly to the road before turning to their destination, as in Fig. 6, they displayed some differences that need to be noted. First, the average lateral distance of pedestrian destination is 5.7 m, and the longitudinal distance is 10.5 m at site 2. The longer lateral distance (3.4 m at site 1) and shorter longitudinal distance (20.4 m at site 1) led to earlier turning toward their destinations, resulting in fewer footprints at the upper left corner and more footprints in the "lower left to upper right" belt. Second, pedestrians at site 2 do not have a median line as a buffer area. Therefore, their footprints in the middle of the road are distributed relatively evenly, as in other positions of the road, which is different with Fig. 6 where an obvious demarcation can be seen at the median line. The modeled position distributions can replicate these differences successfully.

RMSE and R^2 were also calculated for pedestrians at site 2. The road width is 10.5 m (3.5 m $*$ 3 lanes). Therefore, 52 points were used in the calculation with the same computing method, as in site 1. The model has an overall RMSE of 0.96 m and average R^2 of 0.87, which indicate slightly better fitness than that at site 1, considering the bigger lateral distance (the bigger the lateral distance, the more difficult the prediction is; see Fig. 7).

Pedestrians' paths at site 2 have four types:

Type b (2 pedestrians, RMSE of 1.21 m, R^2 of 0.75);
Type c (15 pedestrians, RMSE of 0.72 m, R^2 of 0.90);
Type d (5 pedestrians, RMSE of 0.81 m, R^2 of 0.80);
Type f (8 pedestrians, RMSE of 1.07 m, R^2 of 0.92).

Type f is similar to Type d at the starting part, and similar to Type c at the ending part. The Type-a path is not present because, in the current layout, pedestrians' destinations are not right across the road. The absence of the Type e path is also the result of the layout difference. The second part (parallel to the road) of the Type e path is usually at the median line in site 1, but site 2 does not have a median line. Among the present types, Type b, although only two cases were observed, is the type with relatively worse predictions. Similar to the findings at site 1, this shows that path types with more turns (2) are more difficult to predict because the transient destinations are in the pedestrian's mind, which cannot be directly observed. The predictability for the other path types do not differ much.

Overall, the validation results at site 2 confirmed that the model is promising in predicting pedestrians' paths under different layouts in terms of road characteristics, vehicle volume, and pedestrian volume, etc.

V. Conclusion

This paper has modeled pedestrian crossing paths at the unmarked roadway in China. It opened the black box of street crossing behavior by considering pedestrians as active decision-makers trying to minimize discomfort by weighing PR with efficiency. Compared with previous models, the model has the following features. First, it focuses on the crossing behavior instead of the free-walking behavior, where no moving obstacles are present. Second, the context is the unmarked roadway instead of signalized crosswalks where behaviors are more rigid due to signal restrictions. Third, vehicles in multiple lanes were incorporated rather than considering only one vehicle or at the one-lane road. Finally, the psychological finding that PR decreased exponentially with gaps [11], [36] was included. These mechanisms can guide pedestrians going toward their destination safely and efficiently. The model was validated with field data, and the modeled paths can repeatedly observed pedestrian paths well in contexts without obvious right-angle turning or large lateral deviations.

The validation results of the model imply that the model may address at least part of the underlying mechanism of crossing the unmarked roadway. Pedestrians get the context information through perception and assess the risk with perceived cues. Then, based on the external risk, they make crossing decision by weighing the external risk with the internal desire of reaching destinations. This process is consistent with previous research. For instance, the gap acceptance behavior [12] indicated the existence of risk assessment, the eagerness of ending waiting [31] implied the desire of reaching destinations, and a previous qualitative model proposed by Ishaque and Noland [28] suggested the tradeoff between the two. The mechanism is theoretically interesting because it considers the pedestrian as an active decision-maker rather than a passive receiver of social [4] or magnetic force [10]. It also enhances our understanding of the computational process in crossing the unmarked roadway rather than treating it as a black box, as in cellular-automata-based simulation models [37].

However, as shown in the model fitness of the five path types, the model did not perform well for pedestrians with right-angle turnings. The sharp turning between obviously different crossing styles seemed to suggest that people planned the paths with several key positions on the road and cross each section separately. In the cyclist path planning model of [38], it is assumed that, before crossing, people made a sketch of the path with temporal destinations. Similarly, a higher level decision-making of the path planning may exist before the reactive decision-making process. In that level, pedestrians observe the crossing site and set their temporal destinations (e.g., the points in Fig. 8) to avoid crossing the wide road at a time. A possible plan is to cross the road in halves, which is already adopted by the model. However, the common turning at the fourth or fifth lane indicated more detailed path planning. Simply using all the temporal destinations as inputs will improve the model fitness, but this input cannot be directly observed in practice. Therefore, modeling of the temporal destinations is needed to address the planned path.

In practice, the proposed model has two potential applications. First, it can be applied in both real-time (online) and offline prediction of pedestrian paths at the unmarked roadway. Real-time prediction needs an updated input of the first drivers' distance to the pedestrian in all lanes; hence, it can be used in improving existing driving simulators. The model can generate realistic pedestrian paths in the context of street crossing with the given destination and other road information. This is meaningful considering that many simulation tools have an accurate presentation of drivers but only have rigid and limited movement control of pedestrians. For instance, STISIM is a commonly used driving simulator, and there are studies that used this tool to explore driver behavior when pedestrians are present [39], [40]. However, the pedestrians in this tool can only have four walking directions (forward, backward, left, and right) with constant speed that is not related to vehicle behaviors [41]. If the current proposed model could be used in the pedestrian simulation part, the pedestrians could flexibly change speed and direction based on the vehicle behaviors. The more realistic pedestrian behaviors can improve the ecological validity of these simulation studies.

In offline cases, the real-time distance between vehicles and pedestrians are not available; therefore, the exact pedestrian path cannot be generated. However, general footprint pattern of most pedestrians (see Fig. 6) can be obtained through simulation. The destinations and start points can be simulated by inputting values within the range that cover the width of the entry and exit sides in the crossing site. The real-time information of the headmost vehicles can be simulated by incorporating vehicle time gap distribution that can vary across sites. The simulation results can help to predict the scope of pedestrian–vehicle conflict area and discover general patterns of pedestrian paths, which are important information for further detailed study of a site. Fig. 10 is an illustration of the input and the output implemented via Visual Basic Applications in Excel.

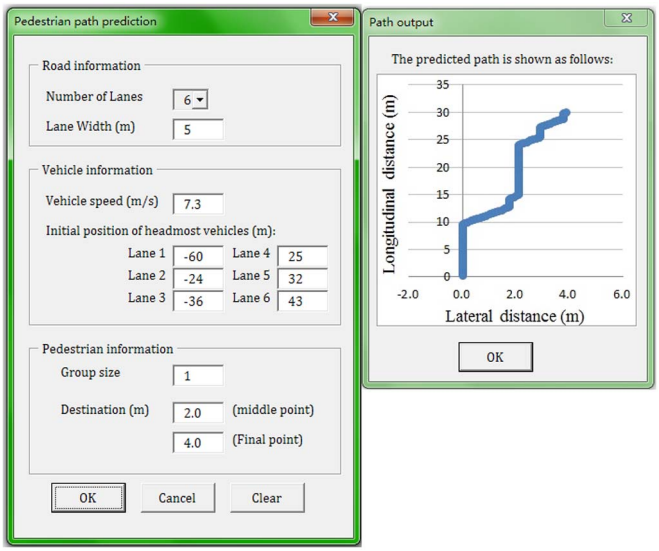

Fig. 10. Prediction of pedestrian paths with offline input.

The left image shows the input, and the right shows the result of one run of the model.

Second, the current model has the potential to facilitate the building of pedestrian protection systems. As reviewed in [42], active pedestrian protection systems track the detected pedestrians via computer vision systems and sensors, and send detection results to the collision prevention module. Then, the system sends cautionary signals or emergency alarms to drivers depending on the predicted danger. The model can be applied to facilitate these systems in two aspects. In the trajectory tracking phase, it can help trajectory estimation in case of failures in the computer vision system and sensors. In this case, the detected points on the road may be not close enough to constitute a smooth trajectory and the missed points can be estimated based on the model. In the collision prediction phase, pedestrian models are at the core of the collision prevention module [42]. However, the reviewed modeling works are mostly movement models [5] that are used in a vehicle-free context and machine-learning-based models that are used in fixed settings [43], [44]. Considering the road-crossing context, the decision-making mechanism introduced in the current model might be used to predict the sporadic pedestrian behaviors in the collision prevention modules.

The applications of the model need more work due to several limitations that need to be addressed in our upcoming work. First, as mentioned before, the modeling of the higher level path planning is needed to get the temporal destinations. Temporal destinations only existed in pedestrians' minds; therefore, it should be estimated in controlled experiments instead of field observations. Second, the model only focused on the path prediction for the "average" pedestrian but neglects pedestrian instant velocities, which are more difficult to predict based on the current inputs of the model because of the sensitiveness to individual differences. The term "capability" in (1) was neglected for the path prediction of an "average" pedestrian but should be considered for velocity issues. For instance, elderly pedestrians are likely to have a speed set that has low speeds, whereas young pedestrians with more capability can have more choices among speed sets. To include the capability information, future works can combine data-based prediction and human decision-making. It is expected to obtain the preferred speed of a pedestrian in the initial crossing period when pedestrians begin their crossing and to use the learned parameter for later predictions with the model. Third, the model emphasizes pedestrian behavioral responses to vehicles but gives relatively less attention to vehicle response to pedestrian behaviors. In China, it is illegal for pedestrians to cross at the unmarked roadway [45]. As the legal road users, drivers have less responsibility for accidents involving a pedestrian compared with that at the crosswalk; thus, they are reluctant to change their speed and direction to respond to pedestrians at unmarked roadways. On the contrary, it is the pedestrians who are hesitant to cross, and thus usually stop or go backward during crossing [46]. Therefore, it is assumed that drivers do not respond to pedestrians as pedestrians cross the road. However, better predictability can be expected if this assumption is relaxed. A possible approach in the next stage of our modeling work is to consider the vehicle speed as a function of its current speed, the relationship with following and leading vehicles, time gaps for approaching pedestrians, and the number of pedestrians ahead. Studies about whether driver will yield to pedestrian [16] may offer ideas about this work. Finally, as a primitive model of a common pedestrian crossing at the unmarked roadway, group proxemics that describes the relationship between pedestrians [47], [48] was not considered. It is hoped that more behavioral mechanism could be included in our final model to consider safety-related behaviors such as walking while using phone, checking approaching vehicles, etc.

APPENDIX
CROSSING BEHAVIOR ANALYSIS

An interview of 12 pedestrians on how they cross an unmarked roadway was conducted to understand the decision-making process. Two findings from the interview are inspiring for the model. First, pedestrians consider wider roads to be more difficult to cross and usually cross it in several trials, mostly by halves. The middle of the road is critical because the source of danger changed from left to right of the pedestrians once they arrived at the median line. Our previous study also found that their waiting time at the median line was similar to that at the starting point in both distribution and duration [24]. This implied that pedestrians may have a transient destination at the median line and a final destination at the end side of the road. Therefore, we assumed that pedestrians cross two halves of the road similarly for simplicity. Second, in the crossing process, pedestrians first look at vehicles and estimate how far (distance) and fast (velocity) the vehicles are traveling. If the time left is sufficient, they will cross very quickly or, otherwise, wait for a better time. This means that, once pedestrians have their destination in mind, they no longer consciously care about the crossing paths. What they really are concerned with is how to get to the destinations safely by adapting their *velocity* to the changing situation. Therefore, reflecting pedestrian paths through velocity over time is an easier and more obvious way than directly addressing the path issue.

ACKNOWLEDGMENT

The authors would like to thank the anonymous reviewers for their valuable suggestions that helped to improve this paper.

REFERENCES

[1] D. R. Geruschat, S. E. Hassan, and K. A. Turano, "Gaze behavior while crossing complex intersections," *Opt. Vis. Sci.*, vol. 80, no. 7, pp. 515–528, Jul. 2003.

[2] S. E. Hassan, D. R. Geruschat, and K. A. Turano, "Head movements while crossing streets: Effect of vision impairment," *Opt. Vis. Sci.*, vol. 82, no. 1, pp. 18–26, Jan. 2005.

[3] D. Helbing, "A mathematical model for the behavior of pedestrians," *Behav. Sci.*, vol. 36, no. 4, pp. 298–310, Oct. 1991.

[4] D. Helbing and P. E. Moln'ar, "Social force model for pedestrian dynamics," *Arxiv preprint cond-mat/9805089*, 1998.

[5] G. Antonini, "A discrete choice modeling framework for pedestrian walking behavior with application to human tracking in video sequences," Ph.D. dissertation, Faculté Sci. Et Tech. De L'ingénieur, École Polytech. Féd. De Lausanne, Lausanne, Switzerland, 2005.

[6] G. Antonini, M. Bierlaire, and M. Weber, "Discrete choice models of pedestrian walking behavior," *Transp. Res. B, Methodol.*, vol. 40, no. 8, pp. 667–687, Sep. 2006.

[7] A. Makarenko, D. Krushinsky, and B. Goldengorin, "Anticipation and delocalization in cellular models of pedestrian traffic," in *Proc. INDS*, 2008, pp. 61–64.

[8] L. Yang, W. Fang, J. Li, R. Huang, and W. Fan, "Cellular automata pedestrian movement model considering human behavior," *Chin. Sci. Bull.*, vol. 48, no. 16, pp. 1695–1699, Aug. 2003.

[9] C. Burstedde, K. Klauck, A. Schadschneider, and J. Zittartz, "Simulation of pedestrian dynamics using a two-dimensional cellular automaton," *Phys. A, Stat. Mech. Appl.*, vol. 295, no. 3/4, pp. 507–525, Jun. 2001.

[10] K. Teknomo, Y. Takeyama, and H. Inamura, "Review on microscopic pedestrian simulation model," in *Proc. Jpn. Soc. Civil Eng. Conf.*, Morioka, Japan, 2000, pp. 536–537.

[11] M. A. Brewer, K. Fitzpatrick, J. A. Whitacre, and D. Lord, "Exploration of pedestrian gap acceptance behavior at selected locations," *J. Transp. Res. Board*, vol. 1982, no. 1, pp. 132–140, 2006.

[12] A. Das, C. F. Manski, and M. D. Manuszak, "Walk or wait? An empirical analysis of street crosssing decisions," *J. Appl. Econom.*, vol. 20, no. 4, pp. 529–548, May/Jun. 2005.

[13] E. Papadimitriou and G. G. Yannis, "Analysis of pedestrian risk exposure in relation to crossing behavior," in *Proc. 91st Annu. Meeting Transp. Res. Board*, Washington, DC, USA, 2012, pp. 1–20.

[14] S. Lassarre, E. Papadimitriou, G. Yannis, and J. Golias, "Measuring accident risk exposure for pedestrians in different micro-environments," *Accident Anal. Prev.*, vol. 39, no. 6, pp. 1226–1238, Nov. 2007.

[15] C. Bonisch and T. Kretz, "Simulation of pedestrians crossing a street," *arXiv:0911.2902v1 [cs.MA]*, vol. 15, 2009.

[16] D. Sun, S. V. S. K. Ukkusuri, R. F. Benekohal, and S. T. Waller, "Modeling of motorist-pedestrian interaction at uncontrolled mid-block crosswalks," in *Proc. 82nd Annu. Meeting Transp. Res. Board*, Washington, DC, USA, 2003, pp. 1–34.

[17] A. Banos, A. Godara, and S. Lassarre, "Simulating pedestrians and cars behaviours in a virtual city: An agent-based approach," in *Proc. Eur. Conf. Complex Syst.*, Paris, France, Nov. 14–18, 2005, pp. 226–230.

[18] M. A. Pollatschek, A. Polus, and M. Livneh, "A decision model for gap acceptance and capacity at intersections," *Transp. Res. B, Methodol.*, vol. 36, no. 7, pp. 649–663, Aug. 2002.

[19] J. A. Michon, "A critical view of driver behavior models: What do we know, what should we do?" in *Human Behavior and Traffic Safety*, R. C. Schwing and L. Evans, Eds. New York, NY, USA: Plenum, 1985, pp. 485–520.

[20] D. L. Strayer and W. A. Johnston, "Driven to distraction: Dual-task studies of simulated driving and conversing on a cellular telephone," *Psychol. Sci.*, vol. 12, no. 6, pp. 462–466, Nov. 2001.

[21] V. Airault and S. Espié, "Behavior model of the pedestrian interaction with road traffic," in *Proc. Eur. Transp. Conf.*, Strasbourg, France, 2005.

[22] S. Moody and S. Melia, "Shared space: Implications of recent research for transport policy," Univ. of the West of England, Bristol, U.K., Working Paper, 2011.

[23] S. Reid, N. Kocak, and L. Hunt, DfT shared space project stage 1: Appraisal of shared space, MVA Consultancy, London, U.K. [Online]. Available: http://assets.dft.gov.uk/publications/shared-space-appraisal/dft-shared-space-project-stage-1.pdf

[24] X. Zhuang and C. Wu, "Pedestrians' crossing behaviors and safety at unmarked roadway in China," *Accident Anal. Prev.*, vol. 43, no. 6, pp. 1927–1936, Nov. 2011.

[25] A. S. Al-Ghamdi, "Pedestrian—vehicle crashes and analytical techniques for stratified contingency tables," *Accident Anal. Prev.*, vol. 34, no. 2, pp. 205–214, Mar. 2002.

[26] "China Road Traffic Accidents Statistics Report of 2004," Traffic Admin. Bureau of China State Sec. Ministry, CRTASR, Beijing, China, 2005.

[27] A. P. Tarko, "Modeling drivers' speed selection as a trade-off behavior," *Accident Anal. Prev.*, vol. 41, no. 3, pp. 608–616, May 2009.

[28] M. M. Ishaque and R. B. Noland, "Behavioural issues in pedestrian speed choice and street crossing behaviour: A review," *Transp. Rev.*, vol. 28, no. 1, pp. 61–86, 2008.

[29] P. C. Fishburn, "Utility theory," *Manage. Sci.*, vol. 14, no. 5, pp. 335–378, Jan. 1968.

[30] S. P. Hoogendoorn and P. H. L. Bovy, "Pedestrian route-choice and activity scheduling theory and models," *Transp. Res. B, Methodol.*, vol. 38, no. 2, pp. 169–190, Feb. 2004.

[31] M. M. Hamed, "Analysis of pedestrians' behavior at pedestrian crossings," *Safety Sci.*, vol. 38, no. 1, pp. 63–72, Jun. 2001.

[32] L. Leden, "Pedestrian risk decrease with pedestrian flow. A case study based on data from signalized interaction in Hamilton, Ontario," *Accident Anal. Prev.*, vol. 34, no. 4, pp. 457–464, Jul. 2002.

[33] U. Gupta, N. Chatterjee, G. Tiwari, and J. Fazio, "Case study of pedestrian risk behavior and survival analysis," *J. Eastern Asia Soc. Transp. Studies*, vol. 8, pp. 2123–2139, Dec. 2010.

[34] T. Wang, J. Wu, P. Zheng, and M. McDonald, "Study of pedestrians' gap acceptance behavior when they jaywalk outside crossing facilities," in *Proc. 13th IEEE Int. Conf. ITSC*, 2010, pp. 1295–1300.

[35] R. Risack, N. Mohler, and W. Enkelmann, "A video-based lane keeping assistant," in *Proc. IEEE Intell. Veh. Symp.*, Dearborn, MI, USA, 2000, pp. 356–361.

[36] J. Cohen, E. J. Dearnaley, and C. E. M. Hansel, "The risk taken in crossing a road," *Oper. Res. Soc.*, vol. 6, no. 3, pp. 120–128, Sep. 1955.

[37] V. J. Blue and J. L. Adler, "Cellular automata microsimulation for modeling bi-directional pedestrian walkways," *Transp. Res. B, Methodol.*, vol. 35, no. 3, pp. 293–312, Mar. 2001.

[38] L. Huang and J. Wu, "Fuzzy logic based cyclists' path planning behavioral model in mixed traffic flow," in *Proc. 11th IEEE Int. Conf. Intell. Transp. Syst.*, 2008, pp. 275–280.

[39] B. H. Kantowitz, "Simulator evaluation of heavy-vehicle driver workload," *Proc. Human Factors Ergonom. Soc. 39th Annu. Meeting*, vol. 39, no. 17, pp. 1107–1111, Oct. 1995.

[40] S. Bromberg, T. Oron-Gilad, A. Ronen, A. Borowsky, and Y. Parmet, "The perception of pedestrians from the perspective of elderly experienced and experienced drivers," *Accident Anal. Prev.*, vol. 44, no. 1, pp. 48–55, Jan. 2011.

[41] "Stisim Help: Stisim Drive (SDL)-PED-Pedestrian," STISIMDRIVE, MIT, Cambridge, MA, USA, 8.29, Jun. 25, 2013. [Online]. Available: http://web.mit.edu/16.400/www/auto_sim/Help/SDLEventPED.htm

[42] T. Gandhi and M. M. Trivedi, "Pedestrian protection systems: Issues, survey, and challenges," *IEEE Trans. Intell. Transp. Syst.*, vol. 8, no. 3, pp. 413–430, Sep. 2007.

[43] F. Large, D. Vasquez, T. Fraichard, and C. Laugier, "Avoiding cars and pedestrians using velocity obstacles and motion prediction," in *Proc. IEEE Intell. Veh. Symp.*, 2004, pp. 375–379.

[44] D. Makris and T. Ellis, "Spatial and probabilistic modelling of pedestrian behaviour," in *Proc. British Mach. Vis. Conf.*, Cardiff, U.K., 2002, vol. 2, pp. 557–566.

[45] "Traffic safety law of the people's republic of China," China State Council, Beijing, China, 2005. [Online]. Available: http://www.gov.cn/banshi/2005-08/23/content_25579.htm

[46] X. Zhuang and C. Wu, "The safety margin and perceived safety of pedestrians at unmarked roadway," *Transp. Res. F, Traffic Psychol. Behav.*, vol. 15, no. 2, pp. 119–131, Mar. 2012.

[47] J. Wás, "Crowd dynamics modeling in the light of proxemic theories," in *Proc. Artif. Intell. Soft Comput.*, 2010, pp. 683–688.

[48] J. J. Faria, S. Krause, and J. Krause, "Collective behavior in road crossing pedestrians: the role of social information," *Behav. Ecol.*, vol. 21, no. 6, pp. 1236–1242, Nov./Dec. 2010.

Xiangling Zhuang was born in Anhui, China, in 1988. She received the B.S. degree in psychology from Zhejiang University, Hangzhou, China, in 2010. She is currently working toward the Ph.D. degree at the Institute of Psychology, Chinese Academy of Sciences, Beijing, China.

She is the author of several journal papers published in *Accident Analysis & Prevention and Transportation Research Part F.* Her main research interests include computational modeling, transportation safety, and intelligent system design.

Changxu Wu (S'04–M'07) received the B.S. degree in psychology, with a focus on engineering and mathematical psychology, from Zhejiang University, Hangzhou, China, in 1999; the M.S. degree in engineering psychology and human–computer interaction from the Chinese Academy of Sciences, Beijing, China, in 2002; and the M.S. and Ph.D. degrees in industrial and operational engineering from the University of Michigan, Ann Arbor, MI, USA, in 2004 and 2007, respectively.

He is the author of more than 35 journal papers published in *Psychological Review*, IEEE TRANSACTIONS ON SYSTEMS, MAN, AND CYBERNETICS–PART A: SYSTEMS AND HUMANS; IEEE TRANSACTIONS ON INTELLIGENT TRANSPORTATIONS SYSTEMS, *ACM Transactions on Computer–Human Interaction*, *International Journal of Human–Computer Studies*, *Acta Psychologica Sinica*, *Ergonomics in Design,* and several other journals. His research interests include integrating cognitive science and engineering system design, particularly modeling human cognition systems with its applications in system design, improving transportation safety, promoting human performance in human–computer interaction, and inventing innovative sustainable and smart energy systems with humans in the loop.

Dr. Wu is a member of the Human Factors and Ergonomics Society, the Society of Automobile Engineers, the Cognitive Science Society, and the American Society of Engineering Education (ASEE). He is an Associate Editor for IEEE TRANSACTIONS ON INTELLIGENT TRANSPORTATIONS SYSTEMS and *Behaviour & Information Technology*. He received the Outstanding Student Instructor Award from the ASEE at the University of Michigan in 2006.